

Calculation of Associated Production of a Top Quark and a W' at the LHC

Edmond L. Berger,¹ Qing-Hong Cao,^{1,2,3} Jiang-Hao Yu,⁴ and C.-P. Yuan^{4,5}

¹High Energy Physics Division, Argonne National Laboratory, Argonne, IL 60439, U.S.A

²Enrico Fermi Institute, University of Chicago, Chicago, Illinois 60637, U.S.A.

³Department of Physics and State Key Laboratory of Nuclear Physics and Technology, Peking University, Beijing 100871, China

⁴Department of Physics and Astronomy, Michigan State University, East Lansing, MI 48823, U.S.A

⁵Center for High Energy Physics, Peking University, Beijing 100871, China

We investigate collider signatures of a top-philic W' model, in which the W' boson couples only to the third-generation quarks of the standard model. The main discovery channel for this W' is through associated production of the W' and top quark, yielding a top-quark pair plus an extra bottom quark jet as a signal. We do a full simulation of the signal and relevant backgrounds. We develop a method of analysis that allows us to conclude that discovery of the W' is promising at the LHC despite large standard model backgrounds. Bottom quark tagging of the extra jet is key to suppressing the backgrounds.

I. INTRODUCTION

Extra charged gauge bosons (W' 's) are present in models of new physics (NP) beyond the standard model (SM) and often assumed to be produced as direct s -channel resonances in hadron collisions. Searches have been carried out at the Tevatron and at the Large Hadron Collider (LHC) for s -channel W' 's in lepton decay modes [1–3], in single top-quark channels [4], and in diboson decays [5].

In this paper we study a different W' model, named a “top-philic” model, in which the W' couples only to third-generation quarks (top and bottom quarks) and is produced only in association with a top quark. It decays only into a top quark and a bottom quark pair. The collider signature of the events is a $t\bar{t}$ pair plus one b -jet. We explore the discovery potential of the top-philic W' boson at the LHC at a center of mass energy of 14 TeV with an integrated luminosity of 100 fb⁻¹. We compute the inclusive cross section, simulate the signal and backgrounds, and investigate a set of optimal cuts. Our study shows that the prospects are promising to discover the top-philic W' in tW' associated production despite the presence of SM backgrounds that exceed our signal by three or four orders of magnitude. The key is to identify as a b jet the extra jet produced in association with $t\bar{t}$. A 1 TeV W' with the same coupling strength as the SM W - t - b interaction could be discovered with a 5 standard deviations statistical significance at the LHC at 14 TeV.

Motivated by the observation of large parity violation in top quark pair-production at the Tevatron [6], several authors have recently proposed a W' boson with a flavor changing d - t - W' interaction [7–9]. This W' boson is also produced in association with a top quark, but it differs from the top-philic W' we discuss in that it decays into a top quark and a non- b quark, yielding a final state of $t\bar{t}$ plus a non- b jet [10]. This final state suffers from a huge $t\bar{t}j$ background that cannot be mitigated by b -tagging on the jet produced in association with the top quark pair. As a result, a large coupling strength would be needed for discovery of the flavor changing W' at the LHC.

II. THE MODEL

A top-philic W' can arise from a new non-abelian gauge symmetry which breaks generation universality [11–13]. A summary may be found in Ref. [14]. In this study we adopt an effective Lagrangian approach rather than focusing on specific NP models. The effective, renormalizable interaction of the W' to the SM third generation fermions is

$$\mathcal{L} = i\frac{g_2}{\sqrt{2}} \bar{t}\gamma^\mu (f_L P_L + f_R P_R) b W'_\mu{}^{++} + \text{h.c.} \quad , \quad (1)$$

where $g_2 = e/\sin\theta_W$ is the weak coupling, while $P_{L/R}$ are the usual chirality projection operators. For simplicity, we consider only the case with a purely left-handed current ($f_L = 1$, and $f_R = 0$), but our study can be extended easily to other cases. The triple gauge interaction of the W' and SM gauge bosons is not included because such a non-abelian interaction is suppressed for large W' mass ($m_{W'}$) by W - W' mixing effects, which are of order $\mathcal{O}(m_W^2/m_{W'}^2)$.

The W' decays entirely to a top quark and bottom quark pair with decay width

$$\Gamma_{W' \rightarrow t\bar{b}} \simeq \frac{3g_2^2 m_{W'}}{48\pi} (f_L^2 + f_R^2) \quad . \quad (2)$$

For $f_L^2 + f_R^2 = 1$, $\Gamma_{W'} \sim m_{W'}/100$, indicating that the W' is quite narrow.

The top-philic W' boson is produced predominately through a gluon-bottom-quark fusion process, as depicted in Fig. 1. The W' decays into a top and bottom quark pair, and the overall final state is then $t\bar{t}b$. Since this final state has not been used to search for a W' at the Tevatron and LHC, none of the current collider limits constrain our top-philic W' model. It is possible the top-philic W' boson could be as light as a few hundred GeV.

The recent CDF measurement of the ratio of the cross sections for $t\bar{t} + 0$ jets to $t\bar{t} + n$ jets is consistent with the SM expectation [15]. Top-philic W' production will contribute to the $t\bar{t} + n$ jets rate. However, our numerical calculation shows that tW' production is too small to be of

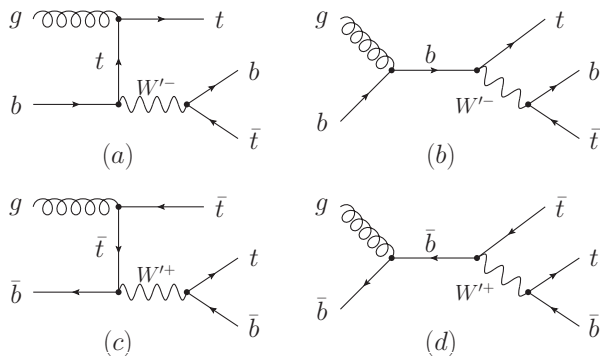


FIG. 1: Feynman diagrams for the associated production of a W' and a top quark: (a, b) W'^-t , and (c, d) $W'^+t\bar{t}$.

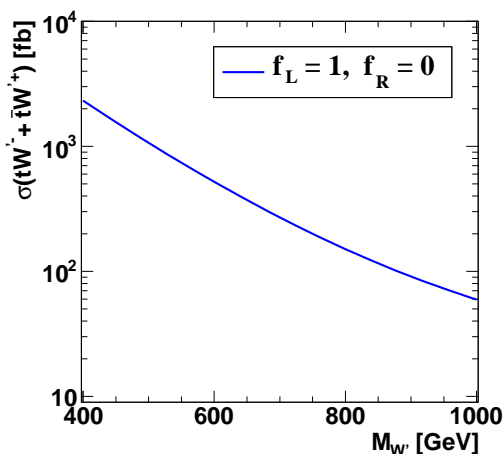


FIG. 2: The inclusive cross section of the tW'^- and $\bar{t}W'^+$ associated production at a 14 TeV LHC with $f_L = 1$ and $f_R = 0$.

concern, e.g. $\sigma(tW'^- + \bar{t}W'^+) \sim 3$ fb for $m_{W'} = 200$ GeV, $f_L = 1$, and $f_R = 0$. Moreover, the cross section drops rapidly with $m_{W'}$. We conclude that the top-philic W' model is consistent with $t\bar{t}$ current measurements at the Tevatron.

In Fig. 2, we display the leading-order inclusive cross section for tW'^- and $\bar{t}W'^+$ production, $\sigma(tW'^- + \bar{t}W'^+)$, as a function of the W' mass ($m_{W'}$) at 14 TeV with a purely left-handed $W'-t$ coupling, i.e. $f_L = 1$ and $f_R = 0$. Note that $\sigma(\bar{t}W'^+) = \sigma(tW'^-)$ owing to equality of the parton distribution functions for initial state b - and \bar{b} -quarks. The CTEQ6L parton distribution functions are used in our calculation with the renormalization and factorization scales chosen as $m_{W'}$. The production cross section is at the picobarn level for a W' with a few hundred GeV mass and at the femtobarn level for a multiple TeV-scale W' .

III. COLLIDER PHENOMENOLOGY

Our signal consists of both tW'^- and $\bar{t}W'^+$ production channels because the two channels give rise to a same $t\bar{t}$ plus one b -jet collider signature after the W' decay. The b -jet could originate from a b or a \bar{b} as one cannot now distinguish b - and \bar{b} -jets experimentally. At the event reconstruction level the b -jet together with one top quark would yield a heavy W' resonance. The main SM background is from production of a $t\bar{t}$ pair plus one b jet. We also take into account the possibility that a light quark jet fakes a b jet. The signal and background events are generated with MadGraph5/MadEvent [18].

In order to trigger on the signal event, we demand a leptonic decay of the top quark $t \rightarrow b\ell^+\nu_\ell$ and hadronic decay of the antitop $\bar{t} \rightarrow \bar{b}jj$. The signal processes are

$$\begin{aligned} pp &\rightarrow tW'^- \rightarrow t\bar{t}b \rightarrow bW^+\bar{b}W^-b \rightarrow b\bar{b}\bar{b}\ell^+jj\nu, \\ pp &\rightarrow \bar{t}W'^+ \rightarrow t\bar{t}\bar{b} \rightarrow bW^+\bar{b}W^-\bar{b} \rightarrow b\bar{b}\bar{b}\ell^+jj\nu. \end{aligned} \quad (3)$$

The topology of our signal is characterized by one isolated positive charged lepton, five high energy jets, and a large missing transverse momentum (\cancel{E}_T) from the missing neutrino. Both electrons and muons are used in our analysis.

We separate the SM backgrounds according to the flavor of the jet produced in association with the $t\bar{t}$ pair:

$$t\bar{t}j : pp \rightarrow t\bar{t}j \rightarrow bW^+\bar{b}W^-j \rightarrow b\bar{b}jj\ell^+\nu, \quad (4)$$

$$t\bar{t}\bar{b} : pp \rightarrow t\bar{t}\bar{b} \rightarrow bW^+\bar{b}W^-b \rightarrow b\bar{b}jj\ell^+\nu. \quad (5)$$

The “extra” jet in association with the $t\bar{t}$ originates from a light-flavor quark or gluon in the first case and from a b or \bar{b} in the second case. As shown below, the two backgrounds are suppressed by different kinematic cuts. In the generation of background events, we demand the transverse momentum (p_T) of the extra jet to be harder than 10 GeV to avoid soft and collinear divergences from QCD radiation. After kinematic cuts, the contributions from other SM backgrounds, e.g. W^+W^-jjj , are quite small and are not included in our analysis.

For an integrated luminosity of 100 fb^{-1} , the numbers of signal and background events at the event generator level are shown in the second column of Table I. The top quark decay branching ratio $\text{Br}(t\bar{t} \rightarrow b\bar{b}\ell^+\nu jj) = 2/27$ is included in the numbers. We choose six benchmark points for the mass $m_{W'}$. We set the $W'-t$ couplings at $f_L = 1$ and $f_R = 0$. The rates for other values of f_L can be obtained from simple scaling

$$\sigma = f_L^2 \times \sigma(f_L = 1). \quad (6)$$

A. Selection cuts

At the analysis level, all the signal and background events are required to pass the *basic* selection cuts listed

TABLE I: The numbers of signal and background events at 14 TeV with an integrated luminosity of 100 fb^{-1} before and after cuts, with $f_L = 1$, for seven values of $m_{W'}$ (GeV). The top quark decay branching ratio $2/27$ is included in the “no cut” column, and the b tagging efficiency is included in the fifth column. The cut acceptances ϵ_{cut} are also listed.

$m_{W'}$	No cut	<i>basic</i>	<i>optimal</i>	<i>b-tagging</i>	ΔM cut	ϵ_{cut}
400	32920	6929	5240	3018	2166	6.6 %
$t\bar{t}b$	1.9×10^5	23849	2712	1537	297	0.15 %
$t\bar{t}j$	3.13×10^7	3×10^6	306062	6984	967	$3.1 \times 10^{-3}\%$
500	15115	3324	2621	1513	1120	7.4 %
$t\bar{t}b$	1.9×10^5	23849	2709	1529	449	0.23 %
$t\bar{t}j$	3.13×10^7	3×10^6	306057	6895	577	$1.8 \times 10^{-3}\%$
600	7361	1666	1300	754	565	7.7 %
$t\bar{t}b$	1.9×10^5	23849	2524	1429	437	0.23 %
$t\bar{t}j$	3.13×10^7	3×10^6	288098	6214	385	$1.2 \times 10^{-3}\%$
700	3843	874	638	369	282	7.4 %
$t\bar{t}b$	1.9×10^5	23849	1781	1026	303	0.16 %
$t\bar{t}j$	3.13×10^7	3×10^6	212153	4441	304	$9.7 \times 10^{-4}\%$
800	2110	490	405	197	154	7.3 %
$t\bar{t}b$	1.9×10^5	23849	1060	620	189	0.10 %
$t\bar{t}j$	3.13×10^7	3×10^6	130122	2346	214	$6.8 \times 10^{-4}\%$
900	1215	290	187	107	85	6.9 %
$t\bar{t}b$	1.9×10^5	23849	594	353	110	0.058 %
$t\bar{t}j$	3.13×10^7	3×10^6	74342	1052	62	$2.0 \times 10^{-4}\%$
1000	720	172	106	62	50	7.0 %
$t\bar{t}b$	1.9×10^5	23849	337	199	64	0.034 %
$t\bar{t}j$	3.13×10^7	3×10^6	42423	505	35	$5.4 \times 10^{-5}\%$

here:

$$\begin{aligned}
p_T^j &\geq 25 \text{ GeV}, & |\eta_j| &\leq 2.5 \\
p_T^\ell &\geq 25 \text{ GeV}, & |\eta_\ell| &\leq 2.5, \\
\Delta R_{jj,j\ell,\ell\ell} &> 0.4, & \cancel{E}_T &> 25 \text{ GeV}
\end{aligned} \tag{7}$$

where p_T denotes the transverse momentum, \cancel{E}_T is the missing transverse momentum from the invisible neutrino in the final state, and ΔR is the separation in the azimuthal angle (ϕ)-pseudorapidity (η) plane between the objects k and l

$$\Delta R_{kl} \equiv \sqrt{(\eta_k - \eta_l)^2 + (\phi_k - \phi_l)^2}. \tag{8}$$

We smear the final state hadronic and leptonic energy according to a fairly standard Gaussian-type detector resolution given by

$$\frac{\delta E}{E} = \frac{\mathcal{A}}{\sqrt{E/\text{GeV}}} \oplus \mathcal{B}, \tag{9}$$

where $\mathcal{A} = 5(100)\%$ and $\mathcal{B} = 0.55(5)\%$ for leptons (jets).

As shown in the third column of Table I, roughly 1/3 of the signal events pass the basic analysis cuts. At this stage, the SM backgrounds are dominant over the signal.

A set of optimized cuts, based on the kinematic differences between the signal and backgrounds, is needed to extract the small signal.

There are five jets in the final state. Jets from a heavy W' boson decay tend to have a harder p_T than jets in the backgrounds. We order the jets by their values of p_T . Jet charge would also be a possibility for labeling jets, but the charge of jets is not well measured experimentally. Figure 3(a) displays the normalized p_T distribution of the jet with largest p_T for a 1 TeV W' . The signal and background curves are normalized by their individual cross sections. The signal distribution (black solid curve) peaks around 450 GeV while the backgrounds peak around 60-80 GeV. The leading jet in the signal is mainly the b -jet from $W' \rightarrow tb$ decay. It shares energy with its top quark partner; therefore its p_T is about $m_{W'}/2$. On the other hand, the leading jet in the backgrounds is predominately from top quark decay. Its p_T spectrum peaks around $m_t/3 \sim 60$ GeV. These distinct p_T spectra motivate a hard cut on the leading jet p_T .

The p_T spectrum of the background is independent of $m_{W'}$, whereas the p_T spectrum of the leading jet in the signal is sensitive to $m_{W'}$. Absent prior knowledge of $m_{W'}$, a first step in a search might be to introduce a mass independent cut to suppress backgrounds, such as to require $p_T > 120$ GeV. This cut could then be increased or decreased to probe for a signal, as we expect experimental collaborations will do to search for heavy resonances.

Since the signal strength is much smaller than the background, we perform Monte Carlo simulations to find the best cut for each $m_{W'}$. This best cut is provided by the simple parameterization

$$p_T^{1\text{st}} \geq \left(50.0 + \frac{m_{W'}}{5}\right) \text{ GeV}, \tag{10}$$

which works well for $400 \text{ GeV} < m_{W'} < 1.0 \text{ TeV}$. We think of these $m_{W'}$ dependent cuts as different cut thresholds. Our $m_{W'}$ dependent cuts are optimized for discovery, and the numbers shown in the fourth column (labeled “optimal”) in Table I should be viewed as optimized results for each $m_{W'}$.

Figures 3(b) and 3(c) show the p_T spectra of the second and the third leading p_T jets. Similar to the leading jet, the 2nd and 3rd leading jets in the signal are harder than those in the backgrounds. We impose kinematic cuts on the 2nd and 3rd jets as follows:

$$\begin{aligned}
p_T^{2\text{nd}} &\geq \left(20.0 + \frac{m_{W'}}{10}\right) \text{ GeV}, \\
p_T^{3\text{rd}} &\geq \left(20.0 + \frac{m_{W'}}{50}\right) \text{ GeV}.
\end{aligned} \tag{11}$$

Another useful variable is H_T , the scalar sum of the p_T 's of all the visible particles in the final state,

$$H_T = p_T^{\ell^+} + \sum_j p_T^j. \tag{12}$$

Figure 3(d) shows the H_T distributions for the signal and backgrounds. Involving a massive W' in the final

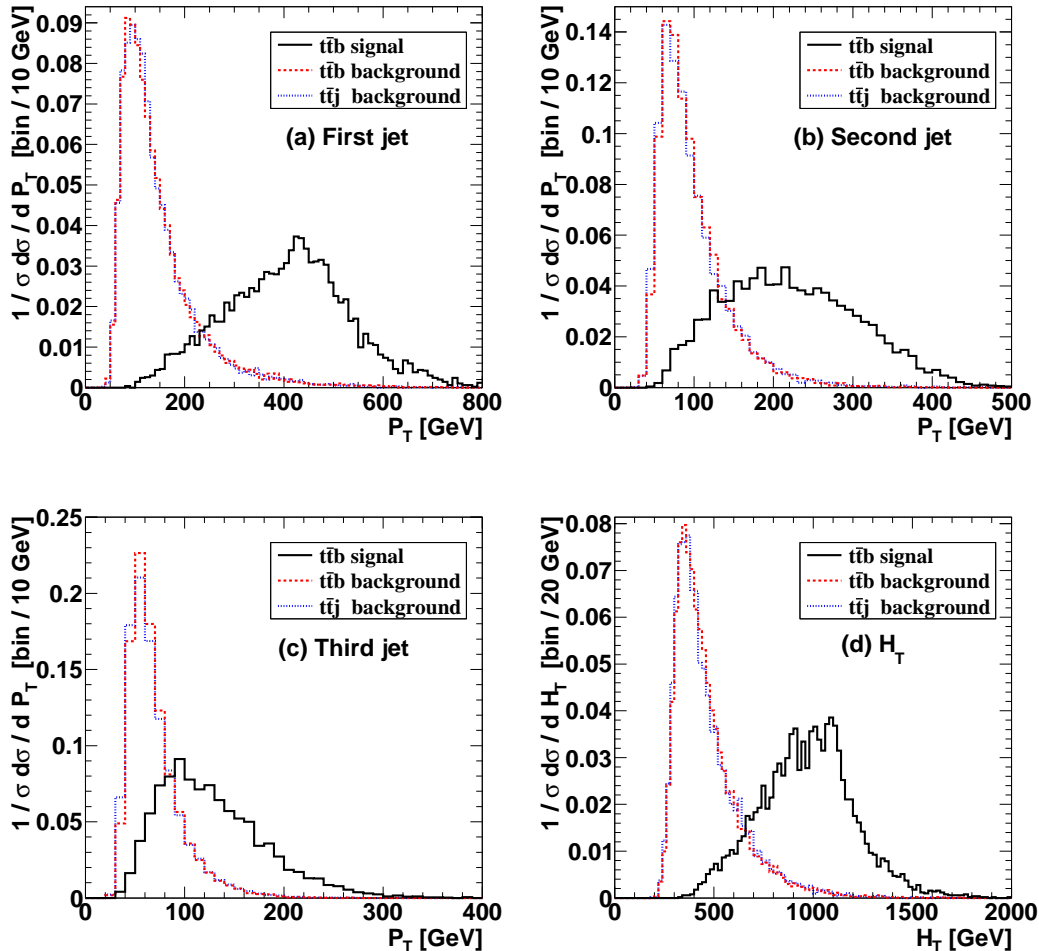


FIG. 3: Normalized p_T distribution of (a) the leading jet, (b) the second leading jet, (c) the third leading jet, as well as (d) the normalized H_T distribution. The black-solid curves represent the signal ($m_{W'} = 1$ TeV), the red-dashed curves the $t\bar{t}b$ background, while the blue-dotted curves the $t\bar{t}j$ background.

state, the signal distribution peaks above 1 TeV while the background distributions peak near the mass threshold of a $t\bar{t}$ pair (~ 400 GeV). This difference enables us to impose a hard cut on H_T to further suppress the SM background:

$$H_T > \left(m_{W'} - \frac{m_{W'}}{10} \right) \text{ GeV}, \quad (13)$$

The fourth column of Table I shows the number of signal and background events after the *optimized* cuts listed in Eqs. (10-13). The $t\bar{t}b$ background is suppressed significantly, but the $t\bar{t}j$ background still overwhelms the signal. However, as we now show, if b -tagging can be applied to the extra jet (the jet produced in association with the $t\bar{t}$ pair), the $t\bar{t}j$ background can be suppressed efficiently. This improvement arises because the extra jet in the signal originates from the b quark in the W' decay while the extra jet in the $t\bar{t}j$ background is from a non- b quark.

B. χ^2 -template and extra-jet tagging

Superficially, the only difference one sees among the final states in Eqs. (3-5) is that the signal and the $t\bar{t}b$ background produce final states with 3 b jets, whereas the $t\bar{t}j$ background has only 2 b jets. The key to suppressing the $t\bar{t}j$ background is to identify the extra b jet in the final state. To do this, we first exploit the difference in p_T between the extra jet and the other jets, and then we require b tagging to identify it as a b jet.

The extra jet in the signal comes from the heavy W' decay and tends to have large p_T . The extra jet in the SM backgrounds, mainly from QCD radiation, tends to have a much softer p_T . However, a complication is that top quarks in the signal events are boosted and jets from top quark decay have large p_T . One of the jets from top quark decay could play the role of the leading jet. Our simulation shows that the extra jet (from heavy W' decay) serves as the leading p_T jet in 62% to 84 % of the

cases for $m_{W'}$ ranging from 400 GeV to 1000 GeV. In view of small signal rate for a heavy W' , a more efficient method is needed to identify the extra-jet.

In this study we use a χ^2 -template method based on the W boson and top quark masses to select the extra jet. For each event we pick the combination which minimizes the following χ^2 :

$$\chi^2 = \frac{(m_W - m_{jj})^2}{\Delta m_W^2} + \frac{(m_t - m_{j\nu})^2}{\Delta m_t^2} + \frac{(m_t - m_{jjj})^2}{\Delta m_t^2} \quad (14)$$

There is two-fold ambiguity in the reconstruction of the longitudinal momentum of the neutrino from top quark decay. Making use of the W -boson on-shell condition, $m_{\nu}^2 = m_W^2$, we can determine the longitudinal momentum of the neutrino ($p_{\nu L}$) as

$$p_{\nu L} = \frac{1}{2p_{eT}^2} \left(A p_{eL} \pm E_e \sqrt{A^2 - 4p_{eT}^2 E_T^2} \right), \quad (15)$$

where $A = m_W^2 + 2\vec{p}_{eT} \cdot \vec{E}_T$. If $A^2 - 4p_{eT}^2 E_T^2 \geq 0$, the value of $p_{\nu L}$ that best yields the known top mass is selected via $m_{\nu b}^2 = m_t^2$. Once detector resolution is taken into account, this ideal situation need not hold. In this case, the value of $p_{\nu L}$ is chosen which yields the minimum χ^2 . The reconstruction efficiencies (ϵ) for a 1 TeV W' compared with Monte Carlo truth are found to be:

$$\begin{aligned} \epsilon_{\text{extra}} &= 99.8\%, \\ \epsilon_{t_{\text{lep}}} &= 98.9\%, \\ \epsilon_{t_{\text{had}}} &= 92.3\%. \end{aligned} \quad (16)$$

Such high efficiencies at the parton level arise mainly from the fact that the jets are highly boosted. Since there are combinatorial ambiguities in the final state, the efficiency for reconstruction of a top quark decaying leptonically (t_{lep}) is higher than for a top quark decaying hadronically (t_{had}).

Once the extra jet is identified by this kinematic method, one can require it to be a b -jet, reducing the $t\bar{t}j$ background by about a half, as is shown in the fifth column of Table I. To retain as many signal events as possible, we require only one jet to be b -tagged. A tagging efficiency of 60% is used in our analysis. We take into account a mistag rate for a light non- b quark (including the charm quark) to mimic a b jet, with mistag efficiency $\epsilon_{j \rightarrow b} = 0.5\%$. For the Monte-Carlo truth events of the signal and backgrounds, we expect that 60% of the signal and $t\bar{t}b$ background events pass the b -tagging, while 0.5% of the $t\bar{t}j$ background events pass the b -tagging. Recall that the $t\bar{t}b$ background is suppressed by the hard p_T and H_T cuts. The b -tagging will further suppress the $t\bar{t}j$ background events with an efficiency 0.5%, if one can perfectly identify the extra-jet out of the five jets in the final state. However, the extra-jet identification with the χ^2 template method is not perfect. The jet identified as the extra-jet has three sources: the true extra-jet, b -quarks from top (antitop) quark decay, and the light-non- b quark from W^- -boson decay. Multiplying the extra-jet

fraction with the corresponding jet-tagging efficiency, we show below that one obtains a net jet-tagging efficiency of 1.2 % for the $t\bar{t}j$ background, cf. Eq. (20), about twice as large as the case of perfect extra-jet identification (0.5 %).

In Table II we show the tagging efficiency $\epsilon_{b\text{-tag}}$ of the extra jet after the χ^2 -template fit. It depends on the reconstruction efficiencies for the extra jet: $\epsilon_{\text{correct}}$ denotes the correct fraction from the χ^2 -fit, $\epsilon_{\text{wrong-}b}$ is the fraction of b jets from top quark decay that fake the extra jet, while $\epsilon_{\text{wrong-light}}$ is the fraction of light jets from top quark decay that fake the extra jet. As an example, consider the b -tagging efficiency in the signal process with 1 TeV W' mass. Since there are five jets in the final state, it is possible that after event reconstruction the extra jet is a b -jet from the top quark or anti-top quark decay (which we label “wrong- b ”), or a light-flavor jet from hadronic top quark decay (which we label “wrong-light”), or a b -jet from the W' decay (which we label “correct”). Note that the b -tagging is applied to the extra jet (which we call “extra-j-tagging”, to avoid confusion with the original b -tagging), but not to the truth b -jet from the W' decay. Taking the reconstruction efficiencies into account, we evaluate the net b -tagging efficiency of the extra jet $\epsilon_{\text{extra-j-tag}}$ as

$$\epsilon_{\text{extra-j-tag}} = (\epsilon_{\text{correct}} + \epsilon_{\text{wrong-}b}) \times 0.6 + \epsilon_{\text{wrong-light}} \times 0.005, \quad (17)$$

for the signal process. A similar analysis gives us the same formula for the $t\bar{t}b$ background. For a 1 TeV W' with hard cuts, we find the extra jet is a b -jet with 99.9% probability, and a light jet with 0.4% probability. Therefore, the b -tagging efficiency for the signal is

$$0.999 \times 0.6 + 0.004 \times 0.005 = 0.60. \quad (18)$$

For the $t\bar{t}j$ background, the correct jet is a light-flavor jet from the real radiation associated with top pair production. The formula changes to

$$\epsilon_{\text{extra-j-tag}} = (\epsilon_{\text{correct}} + \epsilon_{\text{wrong-light}}) \times 0.005 + \epsilon_{\text{wrong-}b} \times 0.6 \quad (19)$$

for the $t\bar{t}j$ background. For the $t\bar{t}j$ background, in the case of a 1 TeV W' with hard cuts, we find extra jet is a light jet with 98.8% probability, and a b -jet with 1.18% probability. Therefore, the b -tagging efficiency for the $t\bar{t}j$ background is

$$0.988 \times 0.005 + 0.012 \times 0.6 = 0.012. \quad (20)$$

We use Eqs. (17-20) to explain the numbers in the b -tagging column in Table II. Table II shows that about 60% of the signal and $t\bar{t}b$ background events pass b -tagging even with the imperfect reconstruction of the extra jet. However, the extra-jet tagging efficiency for the $t\bar{t}j$ background is always larger than the b -tagging efficiency of 0.005 because it always is possible to mistag a b -jet when the extra-jet tagging is done.

TABLE II: The efficiency for extra jet reconstruction with the χ^2 -template method. The net b -tagging efficiencies ($\epsilon_{\text{extra-j-tag}}$), calculated with Eqs. 17 and 19, are shown in the last column.

$m_{W'}$	$\epsilon_{\text{correct}}$	$\epsilon_{\text{wrong-b}}$	$\epsilon_{\text{wrong-light}}$	$\epsilon_{\text{extra-j-tag}}$
400	98.15 %	1.63 %	0.22 %	59.9 %
$t\bar{t}b$	98.34 %	1.5 %	0.15 %	59.9 %
$t\bar{t}j$	96.67 %	2.96 %	0.37 %	2.26 %
500	98.53 %	1.35 %	0.12 %	59.9 %
$t\bar{t}b$	98.34 %	1.5 %	0.16 %	59.9 %
$t\bar{t}j$	96.7 %	2.92 %	0.37 %	2.23 %
600	99.32 %	0.59 %	0.08 %	59.9 %
$t\bar{t}b$	98.34 %	1.48 %	0.15 %	59.9 %
$t\bar{t}j$	96.75 %	2.88 %	0.36 %	2.22 %
700	99.4 %	0.51 %	0.09 %	59.9 %
$t\bar{t}b$	98.6 %	1.27 %	0.12 %	59.9 %
$t\bar{t}j$	97.15 %	2.55 %	0.29 %	2.02 %
800	99.66 %	0.31 %	0.03 %	60 %
$t\bar{t}b$	98.93 %	1.0 %	0.07 %	60 %
$t\bar{t}j$	97.6 %	2.17 %	0.23 %	1.79 %
900	99.87 %	0.12 %	0.01%	60 %
$t\bar{t}b$	99.24 %	0.69 %	0.06 %	60 %
$t\bar{t}j$	98.17 %	1.63 %	0.2 %	1.46 %
1000	99.79 %	0.14 %	0.06 %	60 %
$t\bar{t}b$	99.5 %	0.43 %	0.07 %	60 %
$t\bar{t}j$	98.65 %	1.18 %	0.17 %	1.2 %

C. Mass window ΔM cut

After full event reconstruction, one can compute the W' mass formed from the extra jet and the reconstructed t - or \bar{t} -quark. Since our signal events consist of both tW'^- and $\bar{t}W'^+$, one half of the signal events exhibit a peak in the invariant mass spectrum of the extra jet and t quark (denoted as m_{tj}) while the other half have a peak in the invariant mass of the extra jet and \bar{t} quark (denoted as $m_{\bar{t}j}$). Figure 4 shows the reconstructed m_{tj} and $m_{\bar{t}j}$ distributions for the signal (red), $t\bar{t}j$ (blue) and $t\bar{t}b$ (green) backgrounds. The signal distribution shows a sharp peak at the input value of $m_{W'}$. The pin shape reflects the narrow width of the top-philic W' boson, e.g. the W' width is about 8 GeV for a 1 TeV W' . The long tail into the small mass region comes from the one-half wrong combination. The peaks of the background distributions around 800 GeV are caused by the combination of hard kinematic cuts and jet identification (with combinatorial factors included).

Once $m_{W'}$ is known, we can impose cuts on m_{tj} or $m_{\bar{t}j}$ to further suppress backgrounds. We first demand large invariant masses for both tj and $\bar{t}j$,

$$m_{tj} > 250 + \frac{m_{W'}}{4}, \quad m_{\bar{t}j} > 250 + \frac{m_{W'}}{4}, \quad (21)$$

and that one of the following two mass window cuts be

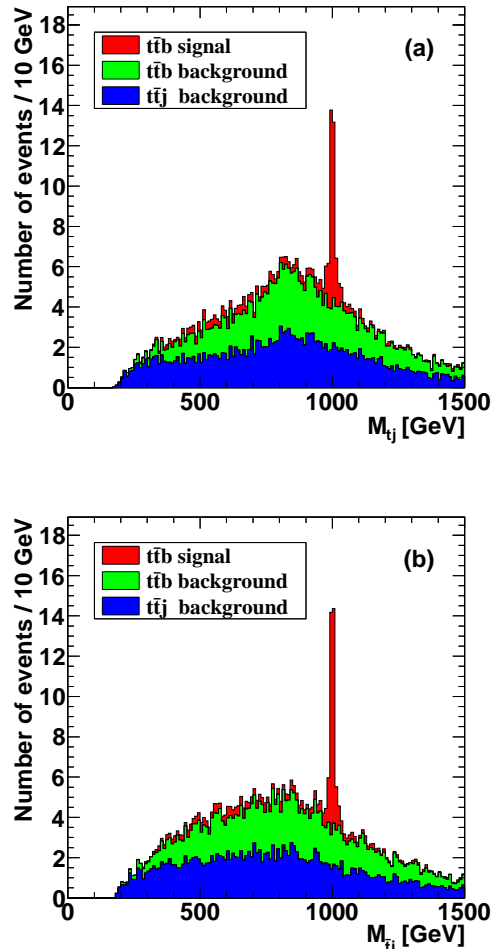


FIG. 4: (a) Reconstructed invariant mass distribution of the leptonic decaying top and extra jet; (b) reconstructed hadronic decaying top and extra jet invariant mass distribution.

satisfied,

$$|m_{tj} - m_{W'}| < \frac{m_{W'}}{10}, \quad \text{or} \quad |m_{\bar{t}j} - m_{W'}| < \frac{m_{W'}}{10}. \quad (22)$$

The mass window suppress both SM backgrounds by a factor of 10 while it keeps most of the signal.

D. Discovery potential

The SM backgrounds are suppressed efficiently such that less than 1 background event survives after cuts with an integrated luminosity of 100 fb^{-1} . For a 1 TeV W' with the same coupling strength as the SM $W-t-b$ interaction, we obtain a 5 standard deviations (σ) statistical significance, defined as S/\sqrt{B} where S and B denotes the number of signal and background events, respectively. For a lighter W' , the significance is larger for fixed coupling strength. The 3σ and 5σ discovery curves are

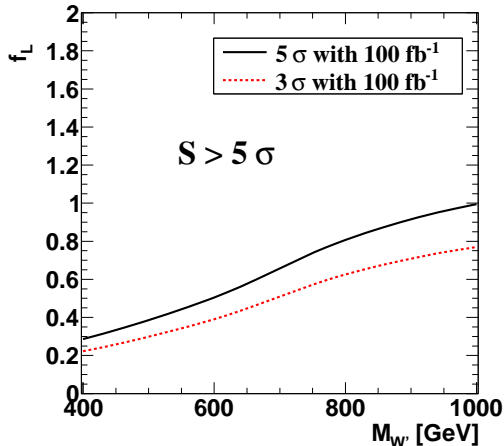


FIG. 5: The discovery potential for the top-philic W' 14 TeV with an integrated luminosity of 100 fb^{-1} .

plotted in Fig. 5. The region above the 5σ curve is good for discovery.

IV. W' - t - b COUPLING AND t -POLARIZATION

After the discovery of this W' boson, one would like to know its mass, spin, and couplings. The invariant mass or transverse momentum distributions of its decay products can be used to determine its mass. Angular distributions of its decay products can be investigated to confirm its spin and the chiral structure of the W' couplings to SM fermions. The chirality of the W' coupling to SM fermions is best measured from the polarization of the top quark [16, 17]. Among the top quark decay products, the charged lepton from $t \rightarrow b l \nu$ is the best analyzer of the top quark spin. For a left-handed top quark, the charged lepton moves preferentially against the direction of motion of the top quark, while for a right-handed top quark the charged lepton moves along the direction of motion of the top quark. The angular correlation of the lepton is $\frac{1}{2}(1 \pm \cos \theta_l)$, with the (+) choice for right-handed and (-) for left-handed top quarks, where θ_l is the angle of the lepton in the rest frame of top quark relative to the top quark direction of motion in the center-of-mass (cm) frame of the incoming partons. In Fig. 6 we plot the $\cos \theta_l$ distribution for $f_L = 1, f_R = 0$ and $f_L = 0, f_R = 1$ couplings. The curves clearly show the main characteristic features of the $\frac{1}{2}(1 \pm \cos \theta_l)$ behaviors for purely right- and left-handed polarized top quarks from W' decay, even after kinematic cuts are imposed. We note that due to the p_T and ΔR cuts, the distributions are distorted and drop significantly in the region $\cos \theta_l \sim -1$ for $f_L = 1$ and $f_R = 0$, and $\cos \theta_l \sim 1$ for $f_R = 1$ and $f_L = 0$. We expect a flat angular distribution for the SM background because the top quark and anti-top quark are not polarized. Therefore, the angular

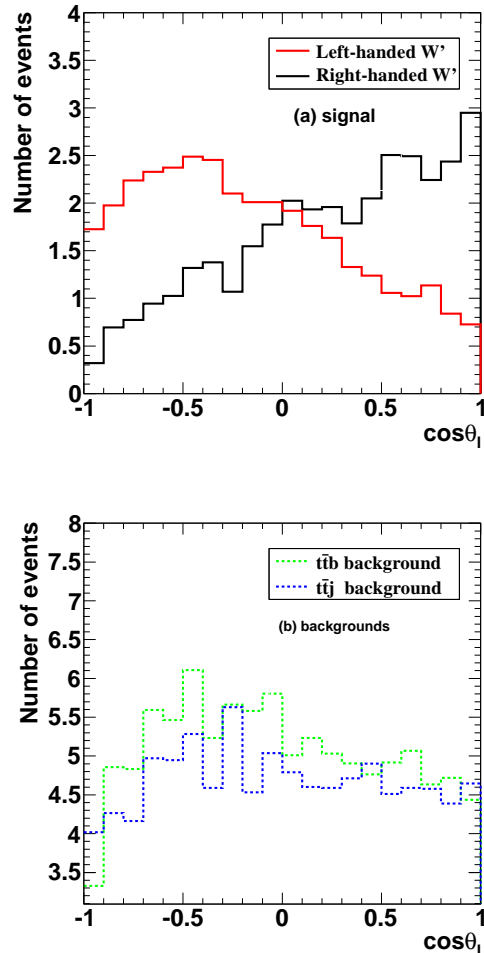


FIG. 6: The angular distributions of the final lepton $\cos \theta_l$ for the left-handed and the right-handed W' .

distributions of the lepton can be used to discriminate top-philic W' models in which the chirality of the W' coupling to SM fermions differs.

V. CONCLUSION

In this paper we examine the LHC phenomenology of a top-philic W' model. In the model the W' boson is produced in association with a top-quark and it decays into a top quark and bottom quark pair, yielding a collider signature of $t\bar{t}$ plus one b -jet. We exploit the different kinematic features of the signal and backgrounds to suppress the large standard model backgrounds from $t\bar{t}j$ and $t\bar{t}b$ production. Examining the distributions of the signal and backgrounds, we find that hard p_T cuts and cuts on H_T can suppress the $t\bar{t}b$ background. After full event reconstruction, we show that tagging the extra b -jet can further suppress the $t\bar{t}j$ background. We show that discovery of a top-philic W' with SM-like coupling

strengths is promising at 14 TeV with $\mathcal{L} = 100 fb^{-1}$. A resonance peak in the top quark and b -jet invariant mass distribution is a distinct signature of W' discovery. Top quark polarization can be used to measure the chiral structure of the W' - t - b coupling. Top quark pair and hard b -jet final states are worth examining even in a model-independent way. This final state is a new unexploited channel at the LHC.

Acknowledgments

The work by E. L. B. and Q.H.C. is supported in part by the U.S. DOE under Grants No. DE-AC02-

06CH11357. Q.H.C. is also supported in part by the Argonne National Laboratory and University of Chicago Joint Theory Institute Grant 03921-07-137. The work by J.H.Y. and C.P.Y. is supported in part by the U.S. National Science Foundation under Grant No. PHY-0855561. E.L.B thanks the Kavli Institute for Theoretical Physics (KITP), Santa Barbara, for hospitality while this research was being completed. Research at KITP is supported in part by the National Science Foundation under Grant No. NSF PHY05-51164. J.H.Y. thanks Reinhard Schwienhorst for discussions of b -tagging and Argonne National Laboratory for hospitality during several visits while part of work was being done.

-
- [1] V. Khachatryan *et al.* [CMS Collaboration], Phys. Lett. B **698**, 21 (2011) [arXiv:1012.5945 [hep-ex]].
- [2] G. Aad *et al.* [ATLAS Collaboration], arXiv:1103.1391 [hep-ex].
- [3] T. Aaltonen *et al.* [CDF Collaboration], Phys. Rev. D **83**, 031102 (2011). [arXiv:1012.5145 [hep-ex]].
- [4] T. Aaltonen *et al.* [CDF Collaboration], Phys. Rev. Lett. **103**, 041801 (2009). [arXiv:0902.3276 [hep-ex]].
- [5] V. M. Abazov *et al.* [D0 Collaboration], arXiv:1011.6278 [hep-ex].
- [6] T. Aaltonen *et al.* [CDF Collaboration], Phys. Rev. D **83**, 112003 (2011) [arXiv:1101.0034 [hep-ex]].
- [7] V. Barger, W. -Y. Keung, C. -T. Yu, Phys. Rev. D **81**, 113009 (2010). [arXiv:1002.1048 [hep-ph]].
- [8] Q. H. Cao, D. McKeen, J. L. Rosner, G. Shaughnessy and C. E. M. Wagner, Phys. Rev. D **81**, 114004 (2010) [arXiv:1003.3461 [hep-ph]].
- [9] V. Barger, W. -Y. Keung, C. -T. Yu, Phys. Lett. B **698**, 243-250 (2011). [arXiv:1102.0279 [hep-ph]].
- [10] M. I. Gresham, I. W. Kim and K. M. Zurek, arXiv:1102.0018 [hep-ph].
- [11] E. Malkawi, T. M. P. Tait and C. P. Yuan, Phys. Lett. B **385**, 304 (1996) [arXiv:hep-ph/9603349].
- [12] X. Li and E. Ma, Phys. Rev. Lett. **47**, 1788 (1981).
- [13] X. G. He and G. Valencia, Phys. Rev. D **66**, 013004 (2002) [Erratum-ibid. D **66**, 079901 (2002)] [arXiv:hep-ph/0203036].
- [14] K. Hsieh, K. Schmitz, J. H. Yu and C. P. Yuan, Phys. Rev. D **82**, 035011 (2010) [arXiv:1003.3482 [hep-ph]].
- [15] T. Aaltonen *et al.* [CDF Collaboration], Phys. Rev. Lett. **102**, 222003 (2009) [arXiv:0903.2850 [hep-ex]].
- [16] E. L. Berger, Q. H. Cao, C. R. Chen and H. Zhang, Phys. Rev. D **83**, 114026 (2011) [arXiv:1103.3274 [hep-ph]].
- [17] S. Gopalakrishna, T. Han, I. Lewis, Z. g. Si and Y. F. Zhou, Phys. Rev. D **82**, 115020 (2010) [arXiv:1008.3508 [hep-ph]].
- [18] J. Alwall, M. Herquet, F. Maltoni, O. Mattelaer and T. Stelzer, arXiv:1106.0522 [hep-ph].